Available online at www.sciencedirect.com

SciVerse ScienceDirect

Procedia CIRP 1 (2012) 347 – 352

www.elsevier.com/locate/procedia

5th CIRP Conference on High Performance Cutting 2012

Numerical Modelling of Vibration-Assisted Turning of Ti-15333

Riaz Muhammad[a,]*, Naseer Ahmed[b], Anish Roy[a], Vadim V. Silberschmidt[a]

a Loughborough University, Wolfson School of Mechanical and Manufacturing Engineering
Loughborough, Leicestershire, LE11 3TU, UK
b Department of Mechanical Engineering, Taibah University, Saudi Arabia
* Corresponding author. Tel.: +44/(0)1509/227566; fax: +44/(0)1509/227502.E-mail address: R.Muhammad@lboro.ac.uk.

Abstract

Rapid developments in the aviation and power industries have stipulated application and development of new high-strength alloys. However, one of the main obstacles on the way to industrial applications of such alloys is their poor machinability. In the recent past, a non-conventional machining technique known as ultrasonically assisted turning (UAT) was introduced; in it low-energy high-frequency vibration is superimposed on movement of a cutting tool. UAT has been used to demonstrate several advantages over conventional turning techniques, especially in the machining of high-strength engineering materials.
In this work, three-dimensional finite element models are developed for both conventional and ultrasonically assisted turning techniques in a commercial code MSC Marc/Mentat. The models were used to investigate the effect of vibration on cutting forces and temperature levels in a cutting region for various cutting conditions. Comparisons of simulations with experimental results demonstrate their predictive capability.

Keywords: Finite elements; UAT; CT; cutting forces; high-strength alloys; Ti- alloys

1. Introduction

Rapid expansion of aviation and power industries in recent decades has led to an increased demand in development and application of new high-strength alloys. Machining of such alloys with conventional techniques can generate high cutting forces and, subsequently, premature tool failure, which leads to increased manufacturing costs, breakdown time on manufacturing lines and poor dimensional accuracy of machined components [1,2].

As a result, new machining techniques need to be developed to process such intractable alloys. Ultrasonically assisted turning (UAT) is a non-conventional machining technique that employs the superposition of high-frequency (f ~ 20 kHz) and low-amplitude (a ~ 15 μm) vibro-impacts on the cutting tool (Fig. 1). The greatest improvement in machining is achieved when vibration is in the direction of the cut [3-6]. Recently, this technique has been introduced commercially in an ultrasonically assisted milling and drilling machine developed by DMG/GildemeisterTM [7].

Numerical simulations are a powerful tool, which can be used to study various physical mechanisms underpinning a material's response to dynamics loads imposed by a vibrating tool. Here, 3D finite-element models of conventional turning (CT) and UAT are developed to study the effects of various machining parameters on the level of cutting forces imposed on the tool and temperature in the cutting region. These simulations are used for comparative analysis of employment of UAT and CT in machining of Ti-15333 alloy.

2. Experimental work

The current UAT setup used in machining experiments consisted of a modified Harrison 300 lathe, with a custom-built ultrasonic transducer mounted on a wave-guide, a force-measurement and data acquisition systems, a charge amplifier and an A/D converter.

 http://dx.doi.org/10.1016/j.procir.2012.04.062

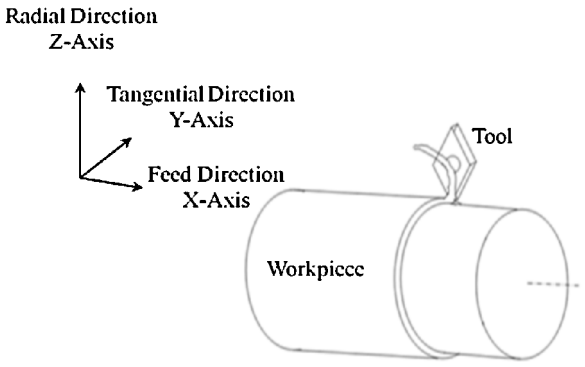

Fig. 1. Directions of principal vibration in ultrasonically assisted turning

The cutting-force components were measured with a Kistler piezoelectric dynamometer (KIAG SWISS Type 9257A), mounted on the cross slide of the lathe using a custom-built tool post. The ultrasonic transducer was mounted on the dynamometer (Fig. 2) with adequate insulation to protect from electrical disturbances, generated during machining operations. Additionally, a micrometric dial gauge is used to ensure an accurate depth of cut.

The cutting conditions used in experimentations are shown in Table 1. An ingot of a β-Ti-based alloy (Ti15V3Cr3Al3Sn) was used as a workpiece material, and a commercial tungsten carbide insert, PVD coated with TiN (DNMG-150608 supplied by Seco) was employed as a cutting tool. All experiments were carried out in dry cutting condition without any lubricant.

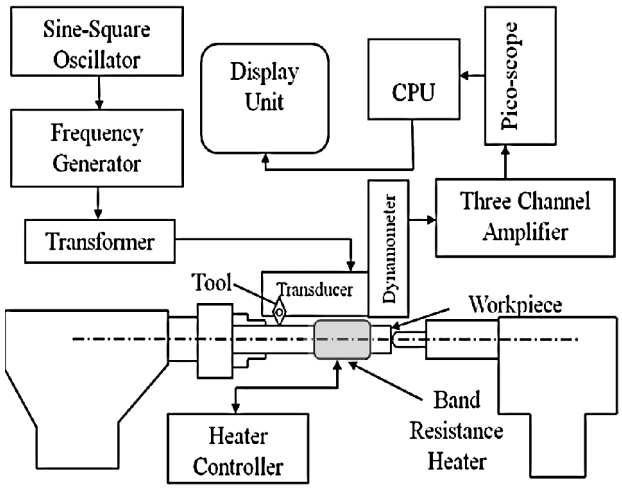

Fig. 2. Schematic diagram of experimental setup for ultrasonically assisted turning

Table 1. Cutting parameters in experiments and FE simulations

Parameters	Value
Cutting speed, V (m/min)	10; 20; 30; 40; 50; 60
Depth of cut, a_p (mm)	0.1; 0.2; 0.3; 0.4; 0.5
Frequency, f (kHz)	20
Amplitude, a (μm)	8

Several tests for CT and UAT were carried out, and the cutting force in cutting direction was measured. Each experiment was repeated at least five times to get statistically consistent data. The cutting forces reduce significantly during ultrasonically assisted operations when compared to those in CT. In general, apart of the force reduction UAT offers substantial benefits, in particular, elimination of the chatter noise during operations and better surface finish [3-6].

3. Description of Finite-Element Models

3D thermo-mechanically coupled finite-element (FE) models of CT and UAT were developed to study deformation processes in high-strength alloys under various cutting conditions by using commercial FE software, MSC MARC/MENTAT. The models were based on an updated Lagrangian procedure that allows for a transient analysis of elasto-plastic materials and accounts for the frictional contact-interaction between the tool and the workpiece.

A schematic of the workpiece and the cutting tool is shown in Fig. 3. For our FE simulations, the model part of deformable workpiece had the following two main dimensions: 3.0 mm in length and 0.7 mm in height. Four-noded iso-parametric elements were used to mesh the workpiece, which were later converted to 4-noded tetrahedral elements as a result of re-meshing of highly distorted elements during the deformation process. Chip separation from the workpiece was achieved through implementation of global re-meshing and rezoning techniques based on the magnitude of penetration and the number of increments of the simulation.

A rigid cutting tool with a tungsten carbide coating moving at a speed (Table 1) is modelled in the FE simulation. In order to simulate UAT, harmonic oscillation in the cutting direction (tangential direction) with an amplitude a = 8 μm and frequency f = 20 kHz was superimposed on the cutting tool's movement. The material properties defined for the cutting tool were those of tungsten carbide that was discretized into eight-noded, 500 iso-parametric, irregular quadrilateral elements with some 400 nodes.

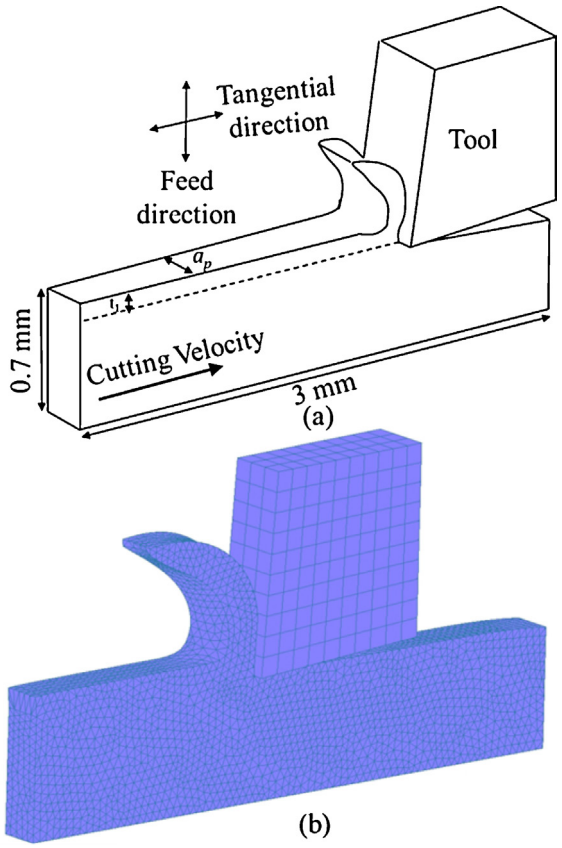

Fig. 3. (a) Schematic of cutting model; (b) fully formed chip with re-meshed body

The ambient temperature was selected as 20°C for the numerical experiments. Also, the effect of friction on the tool-workpiece-interface was incorporated to account for its effect on the cutting forces. Various friction models are reported in the literature [8-12]. For our simulations, a modified shear friction law is believed to adequately represent the friction behaviour at the tool-workpiece-interface [13]. This friction law has the following form:

$$\sigma_{\text{fr}} \leq -m_{\text{fr}} \frac{\bar{\sigma}}{\sqrt{3}} \frac{2}{\pi} \text{sgn}(V_r) \text{artan}\left(\frac{V_r}{V_{cr}}\right), \quad (1)$$

where σ_{fr} is a friction stress, $\bar{\sigma}$ is the equivalent stress, V_r is the relative sliding velocity, V_{cr} is the critical sliding velocity, m_{fr} is the friction coefficient and sgn(x) is the signum function of x.

A piece-wise linear material model was used to represent the response of the Ti-based alloy at various strain rates and temperatures [3, 14]. Figure 4 shows the stress-strain relation for different strain rates obtained from a series of split-Hopkinson tests at elevated temperature of 600°C, carried out at Tampere University of Technology, Finland. The material properties of Ti-15333 are E = 87 GPa, ν = 0.3 and ρ = 4900 kg/m^3, where E, ν and ρ are the Young's modulus, Poisson's ratio and density of the material, respectively. Thermal conductivity of the Ti-15333 is K = 8.08 W/mK. Behaviour of the material with temperature-dependent thermal expansion and specific heat was incorporated into the model; additional details are available elsewhere [14].

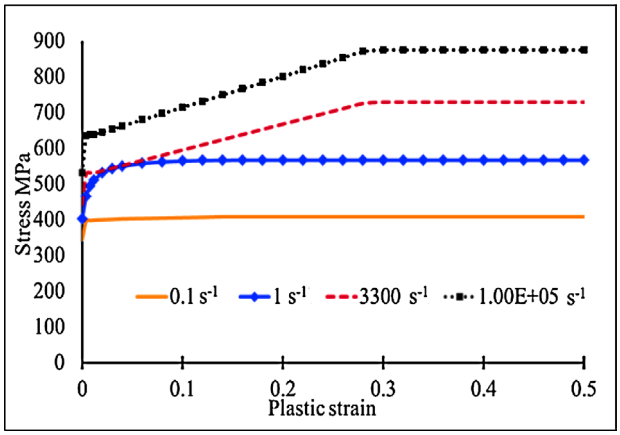

Fig. 4. Modified strain-rate-sensitive material model for Ti-15333 at 600°C [3, 14]

The curves were modified to account for a high-strain-rate response at 10^5 s^{-1} that is estimated to be 20% higher than that for the highest experimental strain rate of 3331 s^{-1}. This estimate was an engineering assumption, and the close match of our numerical results with experimental data demonstrates that the assumption was correct.

4. Results and discussion

Results obtained in our FE simulations of CT and UAT of Ti-15333 are presented and discussed in this section.

A significant reduction in the average cutting forces was observed for cases with application of ultrasonic vibrations. In CT, the cutting tool was in continuous contact with the workpiece, resulting in a constant level of cutting forces after the initial stage of tool engagement, whereas in UAT, the vibrating cutting tool caused cutting force to fluctuate between a maximum (a peak force during penetration) and minimum (no force when the tool is not in contact with the chip). A reduction of 69% in a tangential component of the cutting force was observed for Ti-15333 with the introduction of ultrasonic vibration as shown in Fig. 5. The cutting forces increased with the increase in the depth of cut as expected. The UAT technique was observed to be effective for higher depths of cut with a consistent reduction (65-77%) in the tangential force component (Fig. 6). In UAT, the cutting forces increased with the increase in cutting speed, and the reduction in cutting forces vanished for speed levels beyond 60 m/min as shown in Fig. 7. However, in CT the cutting

forces remain almost the same for various cutting speeds (Fig. 7).

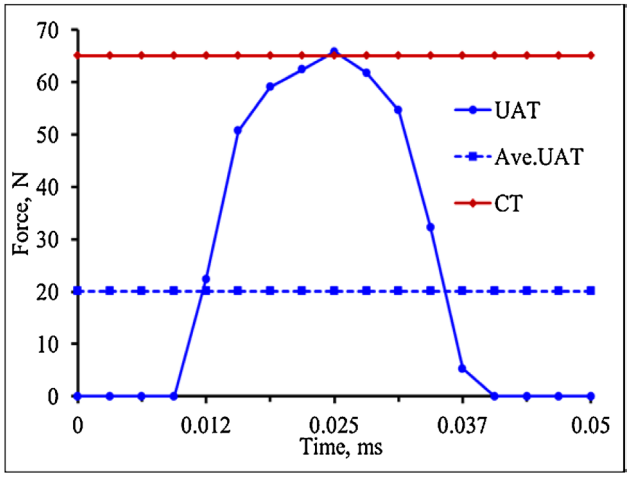

Fig. 5. Tangential components of cutting force in CT and UAT of Ti-15333 (Cutting speed V =10 m/min; depth of cut a_p= 0.2 mm; frequency f = 20 kHz and amplitude a = 8 µm)

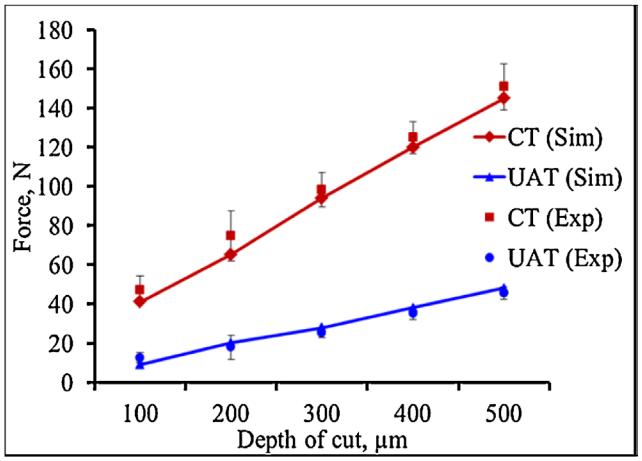

Fig. 6. Tangential component of cutting forces in CT and UAT of Ti-15333 at various depths of cuts and cutting speed V =10 m/min

Higher material removal rates can potentially be achieved in UAT when compared to CT. The cutting force on the tool is 40 N at 100 µm depth of cut in CT, whereas, at a depth of cut of 500 µm in UAT, the observed cutting force is only 44 N. Therefore, for the same level of cutting forces acting on the cutting tool, the material removal rate can potentially be increased to five times in UAT when compared to CT (Fig. 6). Therefore, UAT can prove to be an effective machining technique for the machining of high-strength alloys. Good agreement between experimental results and simulations based on the developed models was observed.

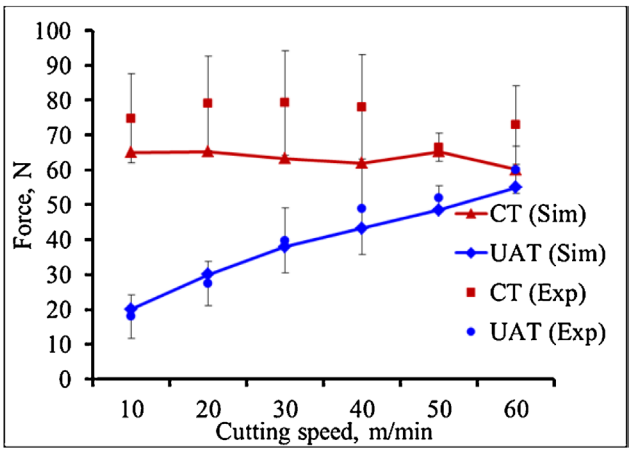

Fig. 7. Tangential component of cutting forces in CT and UAT of Ti-15333 at various cutting speed and depth of cut a_p= 0.2 mm

The calculated distributions of equivalent von-Mises stresses in the cutting regions of the studied alloys for both CT and UAT are shown in Fig. 8. In CT the stress distribution is concentrated mainly in the primary and secondary shear zones. The first of these regions is between the tool-tip and back side of the chip, and second is on the rake-face (front) of the cutting tool. In UAT, the distribution of equivalent von Misses stress is transient and changes with the tool movement. The stress values at the tool-workpiece interaction zone reaches 1040 MPa in CT and remain constant during the process, whereas in UAT, the maximum stress value reaches 1050 MPa at the maximum penetration stage and then reduce to 490 MPa in the unloading stage. As soon as the tool comes into contact with the chip again at the next penetration stage, the value of stresses reaches the peak value and thus the cycle is repeated. However, the average values of the equivalent von-Mises stress in the cutting region in UAT is smaller when compared to CT.

Temperature of the process zone in CT and UAT was also investigated, as shown in Fig. 9. In the simulations of both UAT and CT, a relatively higher temperature was observed along the contact area of tool-workpiece interface. Temperature in UAT is higher when compared to CT at the maximum penetration of the tool, the possible causes for this are the effect of additional factor linked to dissipation of vibration energy [3-6]. However, in UAT the average temperature of the tool remains lower as compared to CT due to the regular separation between the tool and the workpiece.

A noticeable increase in temperature of the cutting region was observed with the increase of cutting speed in both CT and UAT, as expected. Furthermore, analysis of temperature distribution on the rake face of the cutting tool showed that the maximum temperature is reached somewhere in the middle of the cutting edge, with some drops towards the ends of the cutting length

(Fig. 10). This result can be attributed to the convective heat transfer from the rake surface of the tool to the environment.

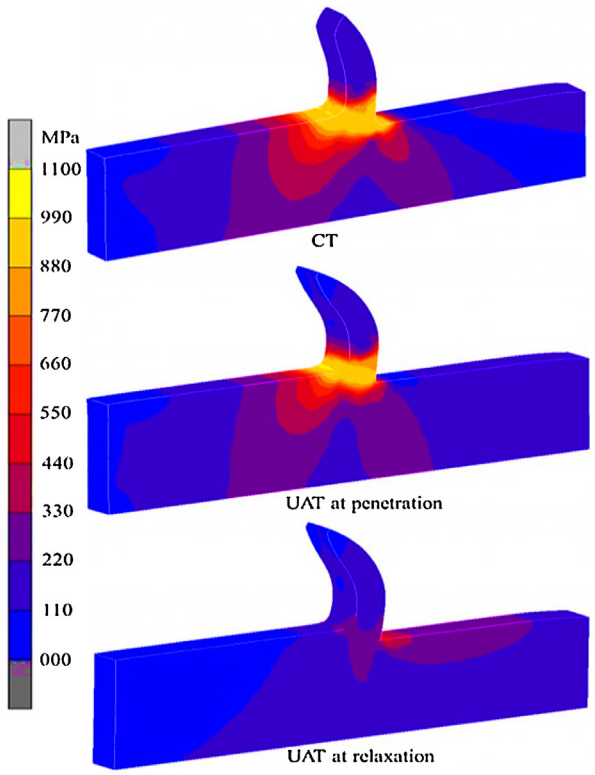

Fig. 8. Equivalent von-Mises stress distribution in cutting region in CT and UAT (at penetration and relaxation stage of ultrasonic vibration)

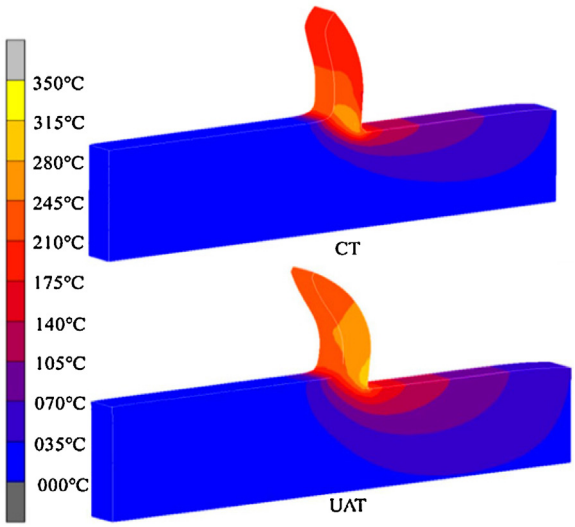

Fig. 9. Temperature distribution in cutting region (depth of cut 0.2 mm; V=10 m/min; frequency 20 kHz and amplitude 8 µm)

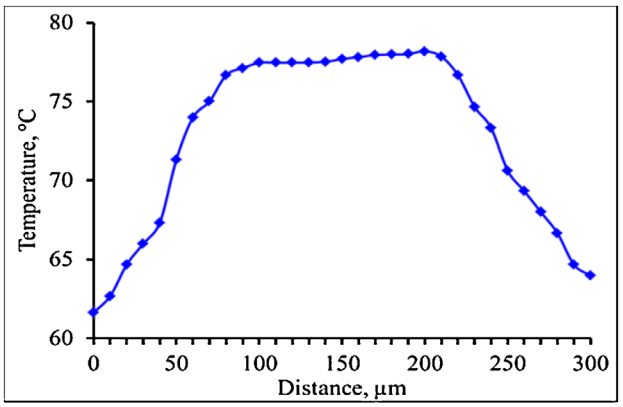

Fig. 10. Temperature distribution on rake face of the tool in UAT

5. Conclusions

A noticeable decline in the average cutting forces was obtained in UAT in comparison to CT: A maximum reduction of 77% in cutting forces was observed in experimentation, with the application of external vibrations to the cutting tool at 200 µm depth of cut and a velocity of 10 m/min, where as in simulation a reduction of 69% was observed for the same cutting conditions. The variance in simulation and experimental results may be an effect of ultrasonic softening in metals and assumptions in the FE simulation. As expected, the cutting forces increases with the increase in the depth of cut. However, UAT is also effective for higher depths of cuts and reduces the tangential cutting forces, considerably. In UAT, the equivalent von-Mises stress values at penetration stage reaches the peak CT values and reduces considerably in the relaxation stage resulting in lower average equivalent von-Mises stresses in UAT when compared to CT.

Temperature in the cutting region in UAT at maximum penetration is higher when compared to CT. However, the average temperature of the cutting tool in UAT is lower when compared to CT. Temperature in the cutting region increases with the increase in the depth of cut and cutting speed, both in CT and UAT.

Potentially, UAT can offer higher material removal rate as compared to CT (up to five times for studied cutting parameters). The numerical model was shown to be in good agreement with the experimental results.

Acknowledgment

The research leading to these results has received funding from the European Union's Seventh Framework Programme (FP7/2007-2013) under grant agreement No. PITN-GA-2008-211536, project MaMiNa.

References

[1] C. R. Dandekar, Y.C. Shin, J. Barnes. Machinability improvement of titanium alloy (Ti-6Al-4V) via LAM and hybrid machining. International Journal of Machine Tools and Manufacture. 2010;50:174-182.
[2] I.A. Choudhury, M.A. El-Baradie. Machinability of nickel-base super alloys: a general review. Journal of Materials Processing Technology 1998;77:278-284.
[3] R. Muhammad, A. Maurotto, A. Roy, V V. Silberschmidt. Analysis of forces in vibro-impact and hot vibro-impact turning of advanced alloys, Applied Mechanics and Materials 2011;70:315-320.
[4] A.V. Mitrofanov, V.I. Babitsky, V.V. Silberschmidt. Finite element analysis of ultrasonically assisted turning of Inconel 718. Journal of Materials Processing Technology 2004; 153-154:233-239.
[5] N. Ahmed, A.V. Mitrofanov, V.I. Babitsky, V.V. Silberschmidt. 3D finite element analysis of ultrasonically assisted turning. Computational Materials Science 2007;39:149-154.
[6] R. Muhammad, N. Ahmed, M. Demiral, A. Roy, V.V. Silberschmidt. Computational study of ultrasonically-assisted turning of Ti alloys. Advanced Material Research 2011;223:30-36.
[7] DMG: DMG D4839/0210ND1; In: Ultrasonic Series; Ultrasonic hard machining and milling on one machine 2010.
[8] G. Shi, X. Deng, C. Shet. A finite element study of the effect of friction in orthogonal metal cutting, Finite Elements in Analysis & Design 2002;38:863-883.
[9] M. Baker, J. Rosler, C. Siemers. A finite element model of high speed metal cutting with adiabatic shearing. Computers & Structures 2002;80:495-513.
[10] R. Muhammad, M. Abid, N. Ahmed, V. Silberschmidt. 3D modelling of drilling process of AISI 1010 steel. Journal of Machining and Forming Technologies 2010; 2 (3-4):201-216.
[11] R. Muhammad, N. Ahmed, Y.M. Shariff, V.V. Silberschmidt. Effect of cutting conditions on temperature generated in drilling process: A FEA approach. Advanced Materials Research 2011;223:240-246.
[12] R. Muhammad, N. Ahmed, Y.M. Shariff, V.V. Silberschmidt. Finite-element analysis of forces in drilling of Ti-alloys at elevated temperature, Solid State Phenomena 2012;188: 250-255.
[13] MSC.Marc User's Guide Version 2011. MSC Software Corporation LA.
[14] M. Demiral, A. Roy, V.V. Silberschmidt, Effects of loading conditions on deformation process in indentation. Computers Materials and Continua 2010; 475(1):1-18.